medRxiv preprint doi: https://doi.org/10.1101/2023.11.27.23299068; this version posted November 28, 2023. The copyright holder for this preprint (which was not certified by peer review) is the author/funder, who has granted medRxiv a license to display the preprint in perpetuity.
All rights reserved. No reuse allowed without permission.

SJPedPanel: A pan-cancer gene panel for childhood malignancies

Pandurang Kolekar[1]*, Vidya Balagopal[2]*, Li Dong[1]*, Yanling Liu[1], Scott Foy[1], Quang Tran[1], Heather Mulder[1], Anna LW Huskey[2], Emily Plyler[1], Zhikai Liang[1], Jingqun Ma[2], Joy Nakitandwe[3], Jiali Gu[2], Jamie Maciaszek[2], Debbie Payne-Turner[2], Saradhi Mallampati[2], Lu Wang[2], Elizabeth Stewart[4], John Easton[1#], Jeffery M. Klco[2#], Xiaotu Ma[1#]

[1]: Department of Computational Biology, St. Jude Children's Research Hospital, Memphis, TN, USA
[2]: Department of Pathology, St. Jude Children's Research Hospital, Memphis, TN, USA
[3]: Department of Laboratory Medicine, Pathology and Laboratory Medicine Institute, Cleveland Clinic, OH, USA
[4]: Department of Oncology, St. Jude Children's Research Hospital, Memphis, TN, USA

*: Contributed equally

[#]: correspondence authors
XM (Xiaotu.Ma@stjude.org); JMK (Jeffery.Klco@stjude.org); JE (John.Easton@stjude.org)

NOTE: This preprint reports new research that has not been certified by peer review and should not be used to guide clinical practice.

medRxiv preprint doi: https://doi.org/10.1101/2023.11.27.23299068; this version posted November 28, 2023. The copyright holder for this preprint (which was not certified by peer review) is the author/funder, who has granted medRxiv a license to display the preprint in perpetuity.
All rights reserved. No reuse allowed without permission.

Abstract

Background

Extensive efforts in the past decade have revolutionized our understanding of the genetic underpinnings of childhood malignancies and identified numerous driver alterations that can provide potential targets for novel therapy and are excellent biomarkers for disease monitoring. For these purposes, a whole genome or exome sequencing approach can be resource prohibitive. Numerous gene panels are developed for adult cancers to address these challenges. Due to the dramatic differences in driver gene landscapes between pediatric and adult cancers, a gene panel for childhood cancers is needed.

Results

Here, we have developed a gene panel dedicated to childhood cancers. This panel (2.82 Mbp) covers 5275 coding exons of 357 driver genes, 297 introns frequently involved in rearrangements that generate fusion oncoproteins, commonly deleted regions, such as *CDKN2A* and *PAX5* (for B-/T-ALL) and *SMARCB1* (for ATRT), and 7,590 polymorphism sites to detect copy number alterations for interrogating tumors with aneuploidy, such as hyperdiploid and hypodiploid B-ALL or 17q gain neuroblastoma. We used driver alterations reported from an established real-time clinical genomics cohort (n=253) to investigate the effectiveness of this gene panel. Among the 485 pathogenic variants reported, our panel covered 417 variants (86%). For 90 rearrangements responsible for oncogenic fusions, our panel covered 74 events (82%). We re-sequenced 113 previously characterized clinical specimens at an average depth of 2,500X using SJPedPanel and recovered 355 (90%) of the 396 reported pathogenic variants. Among the 30 unique genes of the 41 missed alterations, 29 genes are mutated in pediatric cancers with a low frequency (<0.21%) and hence not covered in the panel. We then investigated the power of this panel in detecting mutations from specimens with low tumor content (as low as 0.1%) using cell line-based dilution experiments and discovered that this gene panel enabled us to detect ~80% variants with allele fraction of 0.2%, while the detection rate decreases to ~50% when the allele fraction is 0.1%. We finally demonstrate its utility

medRxiv preprint doi: https://doi.org/10.1101/2023.11.27.23299068; this version posted November 28, 2023. The copyright holder for this preprint (which was not certified by peer review) is the author/funder, who has granted medRxiv a license to display the preprint in perpetuity.
All rights reserved. No reuse allowed without permission.

in disease monitoring on clinical specimens collected from AML patients in morphologic remission.

Conclusions

Overall, our gene panel enables the detection of clinically relevant genetic alterations including rearrangements responsible for subtype-defining fusions for childhood cancers by targeted sequencing of ~0.15% of human genome. Our panel will significantly enhance the analysis of specimens with low tumor burdens for cancer monitoring and early detection.

Keywords

Pediatric cancer, Gene panel, Next Generation DNA sequencing, Genetic testing, Molecular Diagnostics, Cancer Early Detection and Monitoring

medRxiv preprint doi: https://doi.org/10.1101/2023.11.27.23299068; this version posted November 28, 2023. The copyright holder for this preprint (which was not certified by peer review) is the author/funder, who has granted medRxiv a license to display the preprint in perpetuity.
All rights reserved. No reuse allowed without permission.

Background

With the rapid progress in next generation sequencing technology, extensive insights on the genetic underpinnings (i.e., driver alterations) of childhood cancers [1-3] have been uncovered in the past decade. To date, diagnostic sequencing has become part of clinical service in some institutions[4-6]. However, significant cost is associated with whole genome and whole exome sequencing. Most importantly, the broad coverage of whole genome and whole exome sequencing renders it challenging to achieve ultra-deep sequencing that is essential for the analysis of specimen with low tumor burden such as for detecting minimal residual disease and for disease monitoring. Gene panel-based sequencing holds the promise to address these challenges.

Although there have been multiple gene panels designed for adult cancers, such as MSK-IMPACT[6], currently there is no comprehensive gene panel for pediatric cancers. This is important considering the recent pan-cancer study of 1,699 childhood cancers has indicated a dramatic difference between adult and childhood cancers, where 55% of the 142 driver genes in pediatric cancers are not found in adult pan-cancer studies [3]. In this study, 62% of driver alterations in childhood cancers are copy number alterations (CNVs) or structural variations (SVs) whose boundaries typically do not fall in protein coding regions. Indeed, our recent study of oncogenic fusions[7] indicated that 55.7%, 22.5%, and 18.5% of pediatric leukemia, brain, and solid tumors have subtypes defined by oncogenic fusions, for which the DNA breakpoints typically fall into intronic regions. These facts render base pair level ascertainment of driver alterations in childhood cancers challenging by using conventional capture sequencing kits such as exome sequencing and call for a dedicated gene panel for pediatric cancers.

Here, we highlight the prominent features of our recently designed pan-cancer gene panel, SJPedPanel, for childhood cancers by comparison with five existing cancer gene panels. We validate its superior coverage of genes relevant to childhood cancers using a well-described real-time clinical cohort via *in silico* analysis, followed by re-sequencing a subset of these cases for experimental validation. We also demonstrate the power of our gene panel in detecting rare variants using ultra-deep

medRxiv preprint doi: https://doi.org/10.1101/2023.11.27.23299068; this version posted November 28, 2023. The copyright holder for this preprint (which was not certified by peer review) is the author/funder, who has granted medRxiv a license to display the preprint in perpetuity.
All rights reserved. No reuse allowed without permission.

sequencing via serial dilution experiments, as well as disease monitoring in remission samples from acute myeloid leukemia (AML) patients.

Results

Panel design

We designed our panel, which we termed as SJPedPanel, by integrating findings from 44 published tumor-normal paired genomics studies of childhood cancers that spans leukemia, brain, and solid tumor [2-4,8-48]. SJPedPanel includes 1.069 million exonic base pairs from 5,275 coding exons for detecting protein coding mutations in 357 known driver genes for childhood cancers [**Fig. 1a**; see Additional file 1: **Table ST1** and Additional file 2]. To account for the structural variations (SVs) that result in subtype-defining oncogenic fusions for which DNA breakpoints typically fall in intronic regions [7], 1.438 million base pairs from 297 introns of 94 genes (Additional file 1: Table ST1) were included. Moreover, 0.209 million bases from promoter regions were targeted for detecting promoter/enhancer alterations including rearrangements and point mutations (**Fig. 1b**). Several highly recurrent tumor suppressor genes, such as *CDKN2A*, *PAX5*, and *SMARCB1*, were targeted by probes tiling the entire gene region for detecting CNVs. To account for losses of these genes due to structural alterations beyond the gene regions, we extended the target regions to frequent DNA breakpoints by using patient data from ProteinPaint [49] and GenomePaint [50]. Collectively, 2.82 million base pairs were designed for potential SNV, Indel, SV and CNV/LOH driver alterations. Notably, a few known childhood cancer drivers are intentionally excluded due to genomic space considerations. For example, *MECOM* [51] and *GFI1B* [52] are known to be involved in promoter-hijacking alterations and were excluded due to the large space needed to cover the many possible breakpoints.

In addition, 7,590 SNPs were selected for detecting copy number variations and loss of heterozygosity (CNV/LOH) across the genome [see Additional file 1: **Table ST2**]. The median distance between these SNPs is 332 Kb, with 25th and 75th quantile

medRxiv preprint doi: https://doi.org/10.1101/2023.11.27.23299068; this version posted November 28, 2023. The copyright holder for this preprint (which was not certified by peer review) is the author/funder, who has granted medRxiv a license to display the preprint in perpetuity.
All rights reserved. No reuse allowed without permission.

being 60 Kb and 593 Kb, respectively [see Additional file 3: **Fig. S1a**]. Notably, >80% of these SNPs have population frequency between 40% and 60% [see Additional file

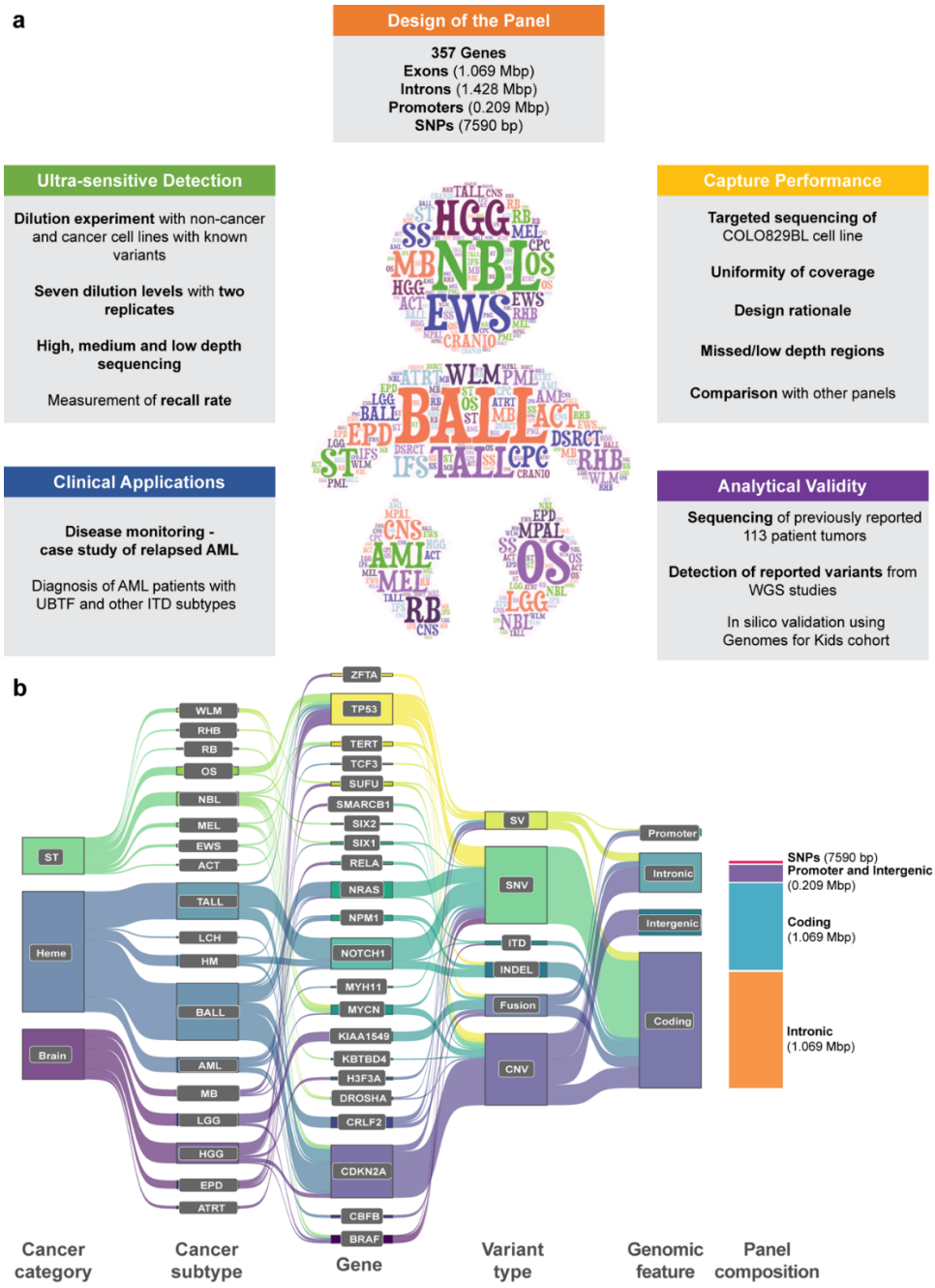

Fig. 1. Design of pediatric cancer gene panel. (a) Study outline, including panel content, investigation of ultra-sensitive detection, capture performance, analytical validity, and clinical applications. (b) A Sankey diagram showing spectrum of childhood cancers (Heme: hematological malignancies; ST: solid tumors; Brain: brain tumors), cancer subtypes, genes, variant types, and genomic features targeted by SJPedPanel. Stacked bar

medRxiv preprint doi: https://doi.org/10.1101/2023.11.27.23299068; this version posted November 28, 2023. The copyright holder for this preprint (which was not certified by peer review) is the author/funder, who has granted medRxiv a license to display the preprint in perpetuity.
All rights reserved. No reuse allowed without permission.

plot at the right end shows space distribution of different genomic features covered by SJPedPanel.

3: **Fig. S1b**], which ensures that that nearly 50% of patients are heterozygous at each SNP site. Therefore, around 3,000 (=7590×0.5×0.8) heterozygous SNPs are expected for each patient, which leads to a theoretical resolution of ~1 Mb for CNV/LOH detection. The number of SNPs chosen per chromosome is roughly proportional to the lengths of chromosomes [see Additional file 3: **Fig. S1c** & Additional file 4]. Considering the read length and the insert length (for target capture and sequencing), these 7,590 SNPs actually occupy ~250*7590=1.8975 million base pairs. Thus, our panel consisted of ~4.7 million base pairs, or ~0.15% of the human genome. The compact size of our panel enables us to reach 30,000X at the cost of a standard WGS (~30X) per sample, thus enabling cost-effective cancer monitoring and/or early detection (**Fig. 1a**). The gene panel was manufactured by Twist Bioscience.

Comparison of gene content with other panels

We first compared the gene content between our panel and five other commonly used commercial panels for childhood cancers, including FoundationOne Heme, FoundationOne CDx [53,54], MSK-IMPACT [6,55], OncoKids [5], and Oncomine Comprehensive assay v3 (OCAv3) [56] (Additional file 1: Supplementary tables ST3a and ST3b). We used the list of 183 driver genes reported in two recent childhood pan-cancer studies [2,3] involving 2,578 cases. As seen in **Table 1**, SJPedPanel covers 159 (87%) genes whereas all other panels covered <60% of the reported pediatric cancer driver genes (**Fig. 2a** and Additional file 1: Supplementary table ST4).

A comparison of gene names among the panels indicated that SJPedPanel has unique coverage of 110 genes (**Fig. 2b**, Additional file 1: Table ST3b) when compared to the other panels combined, such as *DGCR8* and *SIX1* for Wilms tumor [57], *SHH* for medulloblastoma [58], *ZFTA* for ependymoma [22,59], *UBTF*-TD [60] and *PICALM* [60,61] for AML. On the other hand, among the 459 genes specific to other panels, only three genes were reported in two recent pediatric pan-cancer studies with low patient frequencies (*ZNF217: 0.59%, PCBP1: 0.31%, and CARD11: 0.21%*)

medRxiv preprint doi: https://doi.org/10.1101/2023.11.27.23299068; this version posted November 28, 2023. The copyright holder for this preprint (which was not certified by peer review) is the author/funder, who has granted medRxiv a license to display the preprint in perpetuity.
All rights reserved. No reuse allowed without permission.

[2,3]. Collectively, our data indicated that SJPedPanel is a unique resource dedicated to childhood cancers.

Table 1. Overview of the panels selected for comparison.

Panel name	Focus area	No. of genes	Genes screened for			SNPs	%Pediatric cancer driver genes covered out of reported 183 genes†	Publication
			Coding exons	Selected introns	Promoter regions			
SJPedPanel	Pediatric cancers	357	357	94	10	7590	87%	This study
FoundationOne® Heme	Adult blood cancers	418	408	31			57%	He et al., 2016
MSK-IMPACT®	Adult solid tumors	468¶	468	13	1	862	52%	Cheng et al., 2015
OncoKids®	Pediatric cancers	181	137	44	1		49%	Hiemenz et al., 2018
FoundationOne® CDx	Adult solid tumors	324	309	34	1		44%	Whitepaper by Company§
Oncomine™ Comprehensive Assay v3	Adult cancers	161	146	15	1		29%	Hovelson et al., 2015

†: 183 pediatric cancer genes are reported in two recent pediatric pan-cancer studies, Ma et al., 2018 [3] and Grobner et al., 2018 [2]
¶: MSK-IMPACT panel has been reported to consist of 468 genes considering 2 different transcript isoforms for CDKN2A gene, however based on unique gene names MSK-IMPACT panel consists of 467 genes.
§: Sources of content for all the panels are available in Additional file 1: Supplementary Table ST3a

Among the panels compared, the MSK-IMPACT panel has the maximum number of genes (467), of which 137 are exclusive from other panels. Most of these genes are relevant to adult cancers with the highest concentration in adult solid tumors [6,55]. Similarly, FoundationOne Heme panel consists of 418 genes with a focus on adult hematological malignancies [53,62]. OncoKids is the only other pediatric cancer panel under comparison and covers 30 genes that are not included in our panel (see **Fig. 2b** and Additional file 1: Table ST3b). *MECOM* is excluded due to large space needed for the diverse promoter hijacking events [51]. *CALR, RARA* and *SS18* were not included due to lack of pediatric genomics cohort involving these genes. Furthermore, among all the panels, SJPedPanel provides the largest intronic space (297 introns from 94 genes) responsible for rearrangements that generate fusion oncoproteins. Collectively, SJPedPanel offers by far the most comprehensive coverage of genetic alterations for the study of childhood malignancies. Given the significantly lower coverage of pediatric cancer driver genes in other panels and exclusive coverage of 110 genes in SJPedPanel, a comprehensive benchmarking of SJPedPanel with other panels was not possible.

medRxiv preprint doi: https://doi.org/10.1101/2023.11.27.23299068; this version posted November 28, 2023. The copyright holder for this preprint (which was not certified by peer review) is the author/funder, who has granted medRxiv a license to display the preprint in perpetuity.
All rights reserved. No reuse allowed without permission.

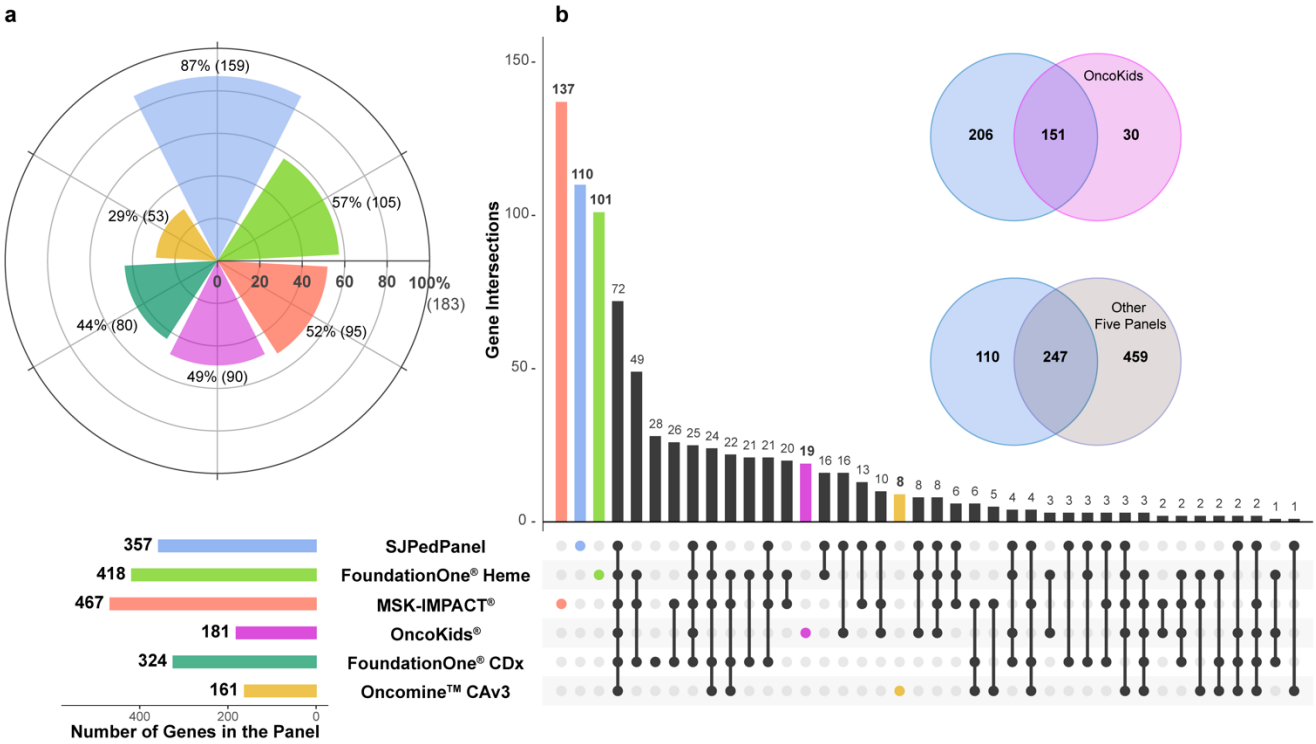

Fig. 2. Comparison of gene content between SJPedPanel with other panels. **(a)** Pediatric cancer relevance of 6 panels based on coverage of 183 driver genes from childhood pan-cancer studies [2,3]. The horizontal bars at the bottom indicate numbers of genes designed in each panel coded by corresponding color. **(b)** Analysis of common and unique genes among 6 panels using UpSet plot [63]. Venn diagrams indicate intersection of SJPedPanel genes with OncoKids, and other fiver panels combined.

Capture performance of the panel

A critical consideration in genomic sequencing, especially in panel sequencing, is the coverage uniformity. To study this question, we sequenced four targeted sequencing libraries (C1- C4) prepared using COLO829BL (ATCC #CRL-1980), a non-cancer cell line that has been extensively used in literature for clinical proficiency testing or benchmarking [64,65]. To ensure reproducibility, technical replicates were generated to achieve high (C1, C2) and low depth (C3, C4) of sequencing. Libraries in each set were sequenced with either the Illumina NovaSeq 6000 (C1, C3, higher throughput, for research sequencing) or NextSeq 500 (C2, C4, medium throughput, for real-time clinical sequencing).

As expected, the average depth was highly correlated (r^2: 0.98) with the number of raw reads sequenced (Additional file 3: Supplementary Fig. S2a). With this data, we

medRxiv preprint doi: https://doi.org/10.1101/2023.11.27.23299068; this version posted November 28, 2023. The copyright holder for this preprint (which was not certified by peer review) is the author/funder, who has granted medRxiv a license to display the preprint in perpetuity.
All rights reserved. No reuse allowed without permission.

investigated the capture uniformity at base pair level (**Fig. 3a-b**) and at region level (**Fig. 3c-d**). Because highly uniform capture data would enable most bases/regions to have similar depth, and therefore a histogram with very small standard deviation, we choose to use coefficient of variation (C_V), defined by σ / μ of the histogram, to measure sequencing uniformity. Here σ and μ are the estimate of standard deviation and mean, respectively, by trimming 2.5% of extreme values from both ends of the histograms (**Fig. 3**). At base pair level, we observed that C_V is close to 0.35 for libraries sequenced by NovaSeq, and to be between 0.37 and 0.38 for libraries sequenced by NextSeq. At region level, NovaSeq data has C_V close to 0.25, while NextSeq data has *Cv* range from 0.22 to 0.28.

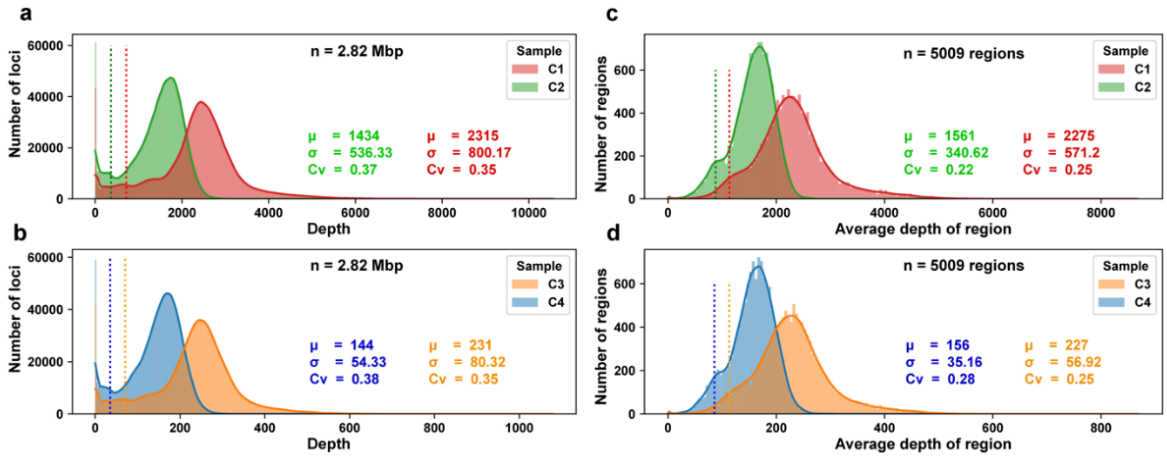

Fig. 3. Capture uniformity per base (a, b) and per region (c, d) of the panel. Uniformity of coverage across ~2.82 million base pairs in the SJPedPanel for high depth samples sequenced on Illumina NovaSeq 6000 (C1) and NextSeq 500 (C2) respectively; and low depth samples sequenced on Illumina NovaSeq 6000 (C3) and NextSeq 500 (C4) respectively. The histograms are made at base pair level **(a, b)** and region level **(c, d)**. The vertical dotted lines indicate (μ -2σ) of the respective distributions. The statistical parameters (μ: average depth, σ: standard deviation, C_v: coefficient of variance) were calculated by trimming observations in upper and lower 2.5 percentiles. All the sample and region level QC parameters are available in the Additional file 1: Supplementary tables ST5 and ST6.

Overall, the standard deviation is less than or around 1/3 of the mean, which ensures that most of the target bases/regions are sufficiently covered. Using the two-sigma rule (that approximates the 95% confidence interval), we also measured the percentage of bases/regions with depth higher than (μ - 2σ). We found that 97% and

medRxiv preprint doi: https://doi.org/10.1101/2023.11.27.23299068; this version posted November 28, 2023. The copyright holder for this preprint (which was not certified by peer review) is the author/funder, who has granted medRxiv a license to display the preprint in perpetuity.
All rights reserved. No reuse allowed without permission.

95% of bases have depth higher than this threshold for NovaSeq data and NextSeq data, respectively (Additional file 1: Table ST5 and Additional file 3: Fig. S2b). Similar trends were observed from the region level analyses (**Figs. 3c-d** and Additional file 1: Table ST6). These data indicated that SJPedPanel has reproducible capture efficiency over different sequencing platforms.

We next analyzed regions that are consistently poorly covered (i.e., less than $\mu - 3\sigma$) in the COLO829 data. We identified such 27 regions (26 regions are small exons), of which 10 regions consistently showed no coverage across all the four samples [see column “Remark” in Additional file 1: Supplementary table ST6]. These 27 regions occupy 8091 bp (~0.3%) of the panel and more than half of these bases (4972 bp) belong to only two regions, *NUTM2A* (3152 bp including intron 1 with 2050 bp) and *DUX4* (1820 bp including exon 1) (see Additional file 1: Supplementary table ST7 and Additional file 3: Supplementary Fig. S3). For *STAG2,* which is well implicated in the pediatric cancers, the coverage is slightly below the pre-defined cut-offs for 3 regions (351 bp) (e.g. ~ 500X for C1 sample, Supplementary table ST7). While looking for the potential reasons for poor coverage of these reasons, we observed that flanking regions (+/- 50 bp) of most of these poorly covered regions comprise either high GC content, such as exon 1 of *MLLT1* (94% GC), or homopolymeric runs, such as T-runs around three regions of *STAG2* gene (see Additional file 1: Supplementary table ST7), which can be informative for future optimization.

Out of the five panels compared, the MSK-IMPACT® panel also reported to have 31 consistently poorly covered regions [55]. Interestingly, SJPedPanel demonstrated sufficient depth of coverage ($> (\mu - 2\sigma)$ of respective COLO829BL sample level cut-offs) for 29 out of the 31 regions (Additional file 1: Supplementary table ST8). The remaining two regions, exon 2 of *NOTCH2* and exon 15 of *PMS2,* were consistently found to show poor coverage as in MSK-IMPACT panel and were also part of the 27 poorly covered regions of SJPedPanel discussed in previous section (Additional file 1: Supplementary table ST7).

Similarly, we analyzed the depth of coverage at designed SNPs. Notably, 99.5% of all the 7590 SNPs have depth more than ($\mu - 2\sigma$) of the respective sample level cut-

medRxiv preprint doi: https://doi.org/10.1101/2023.11.27.23299068; this version posted November 28, 2023. The copyright holder for this preprint (which was not certified by peer review) is the author/funder, who has granted medRxiv a license to display the preprint in perpetuity.
All rights reserved. No reuse allowed without permission.

offs (Additional file 1: Supplementary Table ST9; see Additional file 3: Supplementary Fig. S4a for median and minimum depth of coverages for SNPs). As expected, the minor allele frequencies (MAF) of all the SNPs in control COLO829BL samples were clustered around either 0, 0.5 or 1 (Additional file 3: Supplementary Fig. S4b). A total of 3300 heterozygous SNPs ($0.3 \leq MAF \leq 0.66$) are observed in COLO829BL, supporting the informativeness of our designed SNPs as mentioned above.

In silico comparison of SJPedPanel and WES in a real-time clinical genomics cohort

As stated above (section "Comparison of gene content with other panels"), the comprehensive benchmarking of SJPedPanel with other panels was not possible, so we compared the coverage of reported pediatric cancer alterations using whole exome sequencing (WES). Because whole exome sequencing (WES) is effectively a capture-sequencing kit that targets coding exons of all genes rather than a panel of genes (thus an upper bound of all potential gene panels), we first asked whether our panel could offer comparable coverage of driver alterations (with a focus of coding SNVs and Indels) in pediatric cancers to WES. The recently published "Genome for Kids" (G4K) study[66] reported pathogenic and likely pathogenic (P/LP) variants (called driver alterations hereafter) using three platform sequencing (WGS, WES and RNAseq) from 253 pediatric cases that encompassed 20 cancer subtypes in a real-time clinical genomics setting, thus enabling us to assess the potential of SJPedPanel to cover driver alterations from diverse childhood cancer types. Here we performed *in silico* analysis of regions targeted by SJPedPanel and WES using the curated positions of 485 driver alterations (including SNV/Indel/SV/ITD; Additional file 3: Supplementary Fig. S5a) from the G4K study (see Additional file 1: Supplementary table ST10). SJPedPanel covered 86% of the 485 reported driver alterations as compared to 76% by WES (**Fig. 4a,** last pair of bars for "All" variants with gray background). Because WES is designed for protein coding exons, we next classified the variants into SNV, Indel, Fusion/SV (structural rearrangements that result in fusion oncoproteins), Other SV (structural rearrangements that do not result in fusion oncoproteins but affect cancer driver genes such as disrupting tumor suppressor genes), and ITD, by using the class labels in the G4K study [66]. As

medRxiv preprint doi: https://doi.org/10.1101/2023.11.27.23299068; this version posted November 28, 2023. The copyright holder for this preprint (which was not certified by peer review) is the author/funder, who has granted medRxiv a license to display the preprint in perpetuity.
All rights reserved. No reuse allowed without permission.

expected, WES missed 88% of the Fusions/SV that are enriched in intronic regions, while SJPedPanel covered 82% of these events. On the other hand, while WES was able to detect all the reported driver SNVs and Indels, SJPedPanel missed 7% and 5% of SNVs and Indels, respectively. Interestingly, a re-examination of these SNVs and Indels indicated that their corresponding genes are rarely mutated in childhood cancers (**Fig. 4a**, see Additional file 1: Supplementary table ST10, "Comment" column). Of note, SJPedPanel covered 100% of the ITDs, while WES has missed 13% of these. In fact, the ITDs missed by WES have DNA breakpoints that fall in introns and resulted in duplication of involved exons, such as tandem duplications in *PAX5* [67] and *KMT2A* [68], for which selected intronic regions were designed in SJPedPanel. In particular our panel is able to capture the recently described *UBTF* exonic tandem duplications[60] (see the following section on "Analytical validity of SJPedPanel in Real-Time Clinical Genomics samples").

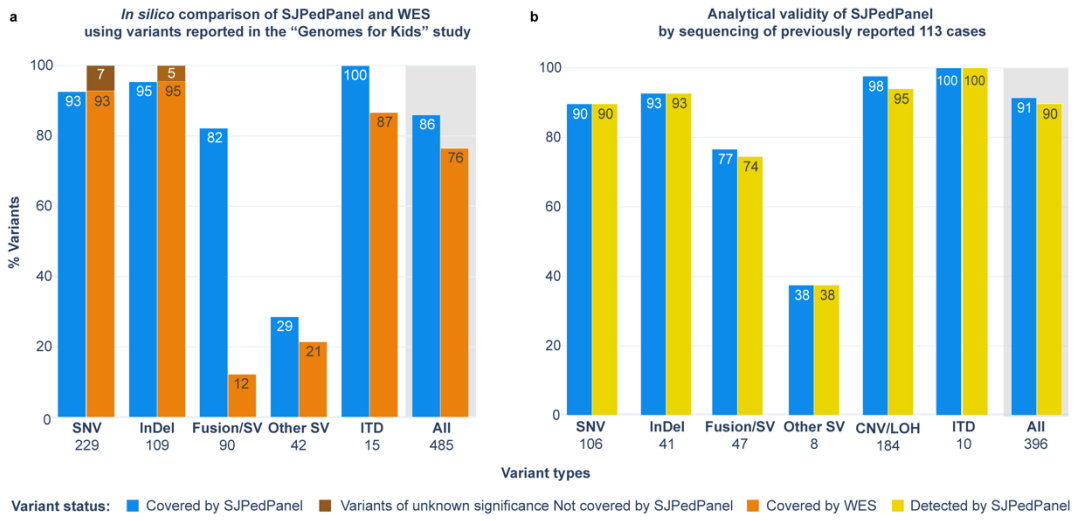

Fig. 4. Coverage comparison with WES and analytical sensitivity of SJPedPanel. (a) *In silico* comparison between SJPedPanel and WES using percent coverage of variants (SNVs, Indels, Fusion, SV and ITDs) reported in the "Genomes for Kids" study. The last pair of bars with gray background for "All" variants show combined percent coverage over all 485 variants. **(b)** Analytical validity of SJPedPanel by sequencing of previously reported 113 cases. Y-axis shows percentage of covered and detected variants by SJPedPanel over each variant type. The last pair of bars with gray background for "All" variants show combined detection rate. Numbers of reported driver alterations are indicated for corresponding variant types.

medRxiv preprint doi: https://doi.org/10.1101/2023.11.27.23299068; this version posted November 28, 2023. The copyright holder for this preprint (which was not certified by peer review) is the author/funder, who has granted medRxiv a license to display the preprint in perpetuity.
All rights reserved. No reuse allowed without permission.

We also asked what percentage of patients could benefit from SJPedPanel vs WES sequencing. As it turned out, at least one variant per case would have been covered by SJPedPanel in 93% of 210 cases with a driver SNV/Indel/SV/ITD (median: 1, range: 1 to 13), in contrast to 75% of the cases using WES (median: 2, range: 1 to 13) (Additional file 3: Supplementary Fig. S5b). Most of this gain is due to the capture of intronic breakpoints that result in oncogenic fusions (Fig. 4a). This data clearly demonstrated that SJPedPanel has superior potential for detection and reporting of driver alterations in pediatric tumors than WES.

Analytical sensitivity of SJPedPanel in Real-Time Clinical Genomics samples

To validate above *in silico* findings, we re-sequenced 113 clinical cases with available specimen from previous clinical studies [4,66] using SJPedPanel. These samples reflect the broad tumor types and subtypes common in childhood cancer, including 27 hematological malignancies, 43 solid tumors and 43 brain tumors (see Additional file 1: Supplementary table ST11 for cohort description). Common subtypes, such as AML (n=14), ALL (n=10), rhabdomyosarcoma (n=5), neuroblastoma (n=5), osteosarcoma (n=3), Wilms tumor (n=3), high-grade glioma (n=8) and medulloblastoma (n=14) are represented in addition to rare entities, such as melanoma (n=1) and desmoplastic small round cell tumor (n=2) (see Additional file 3: Fig. S6). Among these cases, 396 driver alterations are reported via three-platform (WGS, WES, RNAseq) sequencing. These include 106 SNVs, 41 Indels, 55 SVs, 184 CNV/LOHs and 10 ITDs (Additional file 1: supplementary tables ST12-ST16). Of these, 362 (91.4%) variants were targeted by the panel, including 95 SNVs (89.6%), 38 Indels (92.7%), 36 Fusion/SVs (76.59%), 3 other SVs (37.5%), 180 CNV/LOHs (97.82%), and 10 ITDs (100%) (**Fig. 4b**, Additional file 1, Table ST17). Of the 34 P/LP variants not covered by our panel (Additional file 1, Table ST17), 11 were SNVs, 3 were Indels, 11 were Fusion/SVs (not designed), 5 were other SVs and 4 were focal CNVs. The uncovered variants belonged to 30 genes, which are not mutated in published pediatric pan-cancer cohorts [2,3] except for *COL1A1* that has a low mutation frequency of 0.2% (see Supplementary Table ST4, Additional file 3: Supplementary Fig. S7 and Additional file 1, Supplementary Table ST17) therefore these genes are not included in our panel design.

medRxiv preprint doi: https://doi.org/10.1101/2023.11.27.23299068; this version posted November 28, 2023. The copyright holder for this preprint (which was not certified by peer review) is the author/funder, who has granted medRxiv a license to display the preprint in perpetuity.
All rights reserved. No reuse allowed without permission.

We achieved a mean depth of ~2500X for all the samples tested (Additional file: ST18), which ensures 95% confidence of detection of variants with ≥1% allele fraction (AF) [69]. By using a "rotation control" method [70] coupled with a recently developed Indel/SV genotyping tool (**Method**), we detected 98% (355 of the 362 covered variants; Additional file 1: ST17) of reported driver alterations. SNVs, Indels, ITDs showed detection rate of 100% **(Fig. 4b)**. The Fusion/SVs showed an overall recall rate of 97% (35 out of 36) of the covered alterations. We noticed that only one fusion/SV marker (*RUNX1::RUNX1T1* from the case SJCBF100) that was included in the panel design with single breakpoint in *RUNX1* was missed due to insufficient depth (21X) of coverage (Supplementary Tables ST13 and ST18), therefore poor capture efficiency in certain genomic regions warrants a future study. By contrast, we could detect 38% (3 out of 8) of Other SVs, as rest of the missed SVs had their breakpoints either in intergenic or non-covered regions, which is consistent with a much larger genomic space for breakpoints in tumor suppressor genes. On the other hand, SJPedPanel detected 94.56% of the reported CNV/LOHs (Supplementary Table ST17). Collectively, SJPedPanel detected 90% of the 396 reported driver alterations from these 113 cases (Fig. 4b, pair of last bars with gray background). Of note, at least one variant was detected for 96.5% cases (n=113), with a median of 3 variants per case (Range = 0-16; Additional file 1: Table ST19). Consistent with the *in-silico* analysis (**Fig. 4a**), a comparison of SNV, Indel, SV and ITD variants (n=212 out of 396) discovered using WES indicated that SJPedPanel covers 86% of these variants whereas WES covered 78% (Additional file 3: Supplementary **Fig. S8**). These data confirm the superior performance achieved using SJPedPanel for childhood cancers with a panel size approximately 10% the size of WES.

We also highlight the successes and challenges in panel designing by using structural variants as examples. First, due to the large genomic size of intronic regions that can be involved in oncogenic fusions, inclusion/exclusion of intronic regions involves a difficult balance between panel size and effective coverage of patient population. In our 2023 study of fusion gene pairs involved in 5,190 childhood cancers [7], 72 representative genes are selected for 274 fusion gene pairs and SJPedPanel included 53 of these 72 genes. The maximum mutation frequency of the 19 genes not included (Supplementary Table ST3c) in our panel is 0.1% [7]. Furthermore, inclusion of all relevant introns of all genes involved in oncogenic

medRxiv preprint doi: https://doi.org/10.1101/2023.11.27.23299068; this version posted November 28, 2023. The copyright holder for this preprint (which was not certified by peer review) is the author/funder, who has granted medRxiv a license to display the preprint in perpetuity.
All rights reserved. No reuse allowed without permission.

fusions would need ~8 Mbp (described in Source data file of Fig, 2k-l mentioned in Liu et al., 2023 [7]). With the observation that some genes can have multiple fusion partners (e.g., 40 of the 53 included representative genes have between 2 to 32 partner genes), in our design we intentionally left out some partner genes by relying on common representative genes, which reduced the space from ~8 Mbp (280 introns) to ~1Mbp (156 introns). For example, including only the intronic regions of *KMT2A* allowed us to detect *KMT2A::MLLT1* fusion in pediatric T-ALL patient (SJMLL002) although we did not include *MLLT1* in the panel content (Additional file 3: Fig. S9). Similar examples include the detection of *RUNX1::RUNX1T1* despite the inclusion of *RUNX1* but not *RUNX1T1* introns (~100K base pairs needed) in SJCBF100. Despite this success, structural variants can be challenging to detect when the involved regions are not included, such as an inversion involving *RB1* gene in case SJRB0051 (Additional file 3: Fig. S10) that was missed because the DNA breakpoints fall into an intronic region of *RB1* and none of *RB1* introns are covered (~180 kb are needed to cover all *RB1* introns).

Apart from SV/Fusions, SJPedPanel covers well known ITDs such as *FLT3*, *NOTCH1*, *BRAF* etc. (Supplementary Table ST16). SJPedPanel also provides exclusive coverage of *UBTF* gene that was recently described in pediatric AML [60], although in literature *UBTF* ITDs are typically mistakenly detected as small Indels [3,60,71,72]. For example, our panel successfully detected *UBTF* TDs in two pediatric AML cases (SJAML015373 and SJAML016569; see Additional file 3: Supplementary Fig. S11) [60].

Determining limit of detection

One of the important applications of panel sequencing is disease monitoring, where the tumor burden is typically less than 1% and thus variants are rare and challenging to detect. To investigate the applicability of our panel, we first performed dilution experiments (with 7 concentration ladders 0.1%, 0.2%, 0.5%, 1%, 2.5%, 5%, 10%, and pure normal of 0% and pure cancer of 100%) using 6 pediatric cancer cell lines (697, EW-8, K562, ME-1, MOLM-13, and Rh30) and 1 non-cancer cell line (GM12878) as normal control. These 6 lines collectively contain 26 unique P/LP variants (14 SNVs, 4 Indels, and 8 SVs) [73,74] (Additional file 1: Supplementary Table

medRxiv preprint doi: https://doi.org/10.1101/2023.11.27.23299068; this version posted November 28, 2023. The copyright holder for this preprint (which was not certified by peer review) is the author/funder, who has granted medRxiv a license to display the preprint in perpetuity.
All rights reserved. No reuse allowed without permission.

ST20) and the lack of shared driver alterations allowed for pooled dilutions to reduce the experimental complexity while keeping the diversity of mutation types. For example, at ladder of 0.5%, we mixed 5:5:5:5:5:5:970 cell equivalents from the 6 cancer lines and the normal line, respectively. To ensure sufficient power of detecting variants with low allele fractions, we achieved an average depth of 5,000X for 0.5%, >7,000X for 0.2% and 0.1% dilution concentrations (Method, Additional file 1: Table ST21).

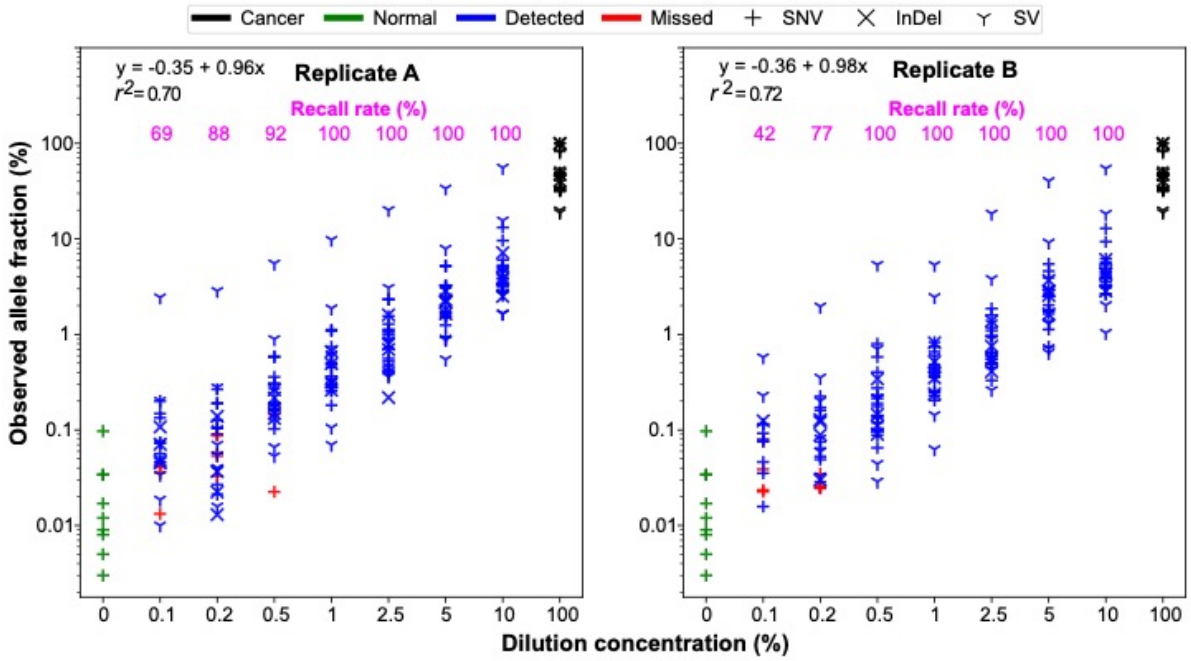

Fig. 5. Determining the limit of detection with SJPedPanel. The observed allele fractions of 26 driver alterations are shown on Y-axis as a function of corresponding dilution concentration shown in X-axis. The detection rate for each dilution concentration is shown on top as magenta text. The observed allele fractions of variants from normal and pure tumor cell lines are also shown using green and black points, respectively. The variants detected with statistically significant Q-values ($Q < 0.05$) are shown in blue, whereas those with insignificant Q-values are shown in red. Shown are results from replicate A (a) and replicate B (b).

We used SequencErr [75] and a newly developed Indel/SV genotyper (manuscript submitted; GitHub: https://github.com/stjude/SVIndelGenotyper) to perform allele counting followed by variant calling using binomial models with false discovery rate control (**Method**), where the pure normal of 0% was used to estimate background

medRxiv preprint doi: https://doi.org/10.1101/2023.11.27.23299068; this version posted November 28, 2023. The copyright holder for this preprint (which was not certified by peer review) is the author/funder, who has granted medRxiv a license to display the preprint in perpetuity.
All rights reserved. No reuse allowed without permission.

error rates as no cancer-driving somatic alterations are expected in non-cancer cell line GM12878. As seen in **Fig. 5**, the observed allele fractions closely represent corresponding dilution ladders, with R-squared values of 0.7 and 0.72, for biological replicates A and B, respectively (Additional file 1: Supplementary table ST22). Notably, although we achieved >90% detection rate when the dilution concentration is above 0.5%, it diminishes quickly at lower dilutions. At a dilution concentration of 0.1%, recall rate was 69% and 42% in replicates A and B, respectively.

To further investigate the effect of sequencing depth on detection rate, we performed *in silico* down-sampling experiment (Method; Additional file 1: Supplementary table ST23). For all the dilutions with concentrations ≥ 1%, which were initially sequenced at 5000X and 2500X (Additional file 3: Fig. S12a and S12b), recall rate is found to be close to 100% even after down sampling their depths to 1000X. However, recall rate declined with down sampled depths for dilution concentrations < 1%. For samples with dilution concentration of 0.5% (Additional file 3: Fig. S12b top panel), recall rate dropped from 97% at 3000X to 75% at 1000X. Thus, recall of markers with allele fraction of 0.5% can be achieved at 2500X~3000X, which is concordant with our theoretical binomial calculation of 2,100X (Method, Fig. 5). However, for markers with allele fraction of 0.2% and 0.1% the detection rate was <50% even at initial 10,000X data (Additional file 3: Fig. S12c). This finding suggests that the current LoD is between 0.1% and 0.5% and is consistent with a recent report using cfDNA data [76].

The above data suggests a depth of 2,100x will ensures 95% chance of detecting >=5 mutant reads if the true allele fraction is >0.5%, However, considering the sequencing uniformity parameter, where 95% of targeted regions are covered at μ-$2\sigma = 0.33\mu$, we would recommend 3 × 2,100 = 6,300X so that >95% of targeted regions will be covered >2,100X and ensure the 95% chance of detecting variants with allele fraction of 0.5%. Since the total space of this panel is ~0.15% of a human genome, 6,300X corresponds to a 9X whole genome sequencing.

medRxiv preprint doi: https://doi.org/10.1101/2023.11.27.23299068; this version posted November 28, 2023. The copyright holder for this preprint (which was not certified by peer review) is the author/funder, who has granted medRxiv a license to display the preprint in perpetuity.
All rights reserved. No reuse allowed without permission.

Case study: Real time tracking of relapsed AML using deep sequencing

To test the suitability of the panel for disease monitoring in a real-world setting, we chose two AML cases (SJAML016582 and SJAML016551) that had remission samples with low tumor content available. These cases have multiple pathogenic and likely pathogenic variants (P/LP) reported by clinical sequencing of diagnosis and relapse samples (Additional file 1: Table ST24) and are ideal for panel sequencing. The remission samples were sequenced to an average depth of 5,000X using SJPedPanel per above power calculations.

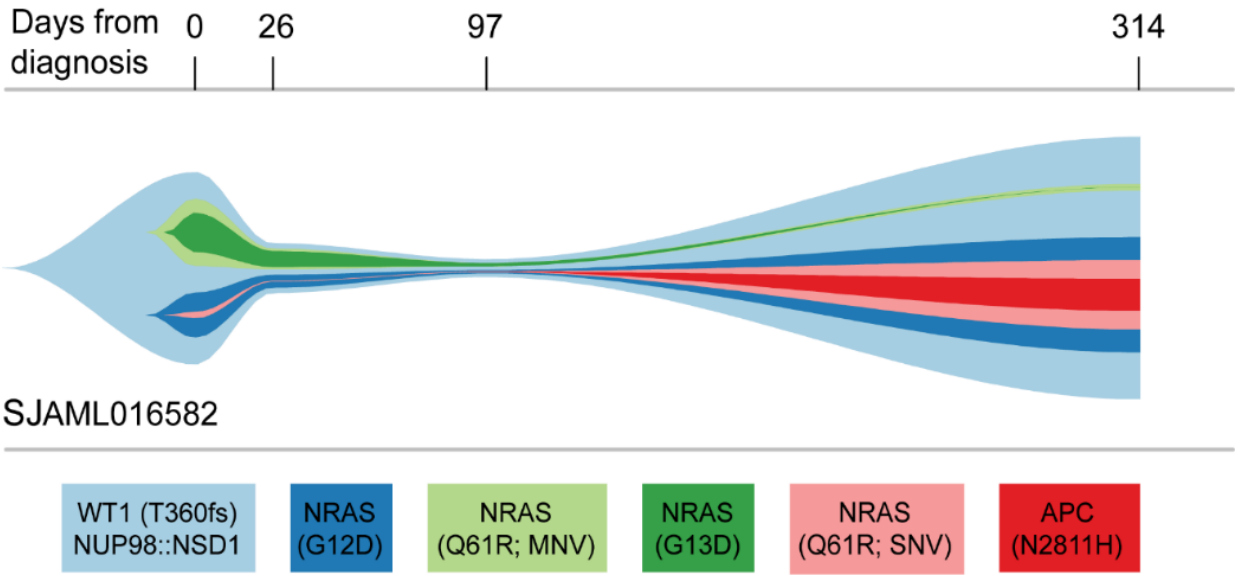

Fig. 6. Real time tumor tracking in case SJAML016582. The estimated cellular fractions of subclones at four timepoints from diagnosis (day 0) to relapse (day 314) are shown as a river-plot. Subclones with very low cellularity (e.g., NRAS Q61R (SNV) at diagnosis) were adjusted for visualization purposes. Actual values are available in the Additional file 1: ST24a.

In case SJAML016582, apart from subtype defining *NUP98*::*NSD1* fusion, 4 pathogenic variants were detected at diagnosis (day 0) and 6 pathogenic variants were detected at relapse (day 315), with 2 variants shared between diagnosis and relapse. With the ultra-deep panel sequencing data, we recovered all variants initially detected by whole genome sequencing, including 4 at diagnosis and 6 at relapse. Interestingly, panel sequencing detected the SNV that encodes *NRAS* Q61R at diagnosis with allelic fraction (AF) 0.12%, and the MNV that encodes *NRAS* Q61R at

medRxiv preprint doi: https://doi.org/10.1101/2023.11.27.23299068; this version posted November 28, 2023. The copyright holder for this preprint (which was not certified by peer review) is the author/funder, who has granted medRxiv a license to display the preprint in perpetuity.
All rights reserved. No reuse allowed without permission.

relapse with AF 0.07%, both of which are beyond the detection power of whole genome sequencing (Additional file 1: Table ST24a; **Fig. 6**). Further, in the day 26 remission data, we detected a high tumor burden (6.56%, Method). Notably, the tumor burden continued to decrease down to AF of 2.88% at day 97 as reflected by the SV responsible for *NUP98::NSD1* fusion.

In addition to disease monitoring, we also applied ultra-deep sequencing for detecting measurable residual disease (MRD) as a measure of patient response to chemotherapy. Generally flow cytometry is a method of choice for such applications [77] in addition to real time PCR [78] and droplet digital PCR [79]. However, these approaches are not as scalable as ultra-deep sequencing. In order to evaluate the efficacy of SJPedPanel to detect MRD, we sequenced three samples from diagnosis (day 0), MRD (day 23) and relapse (day 344) for AML patient SJAML016551. Here the relapse sample is used to definitively define genetic alterations that are present in the MRD sample. For this case, five pathogenic variants, including a *KMT2A::MLLT10* structural variant, were identified to be shared between diagnosis and relapse and are expected to be detected in MRD sample. Although flow-based MRD detection was negative for this case, our deep sequencing detected all 5 pathogenic variants with allele fraction range between 0.7-1% (Additional file 1: Table ST24b; Additional file 3: Supplementary Fig. S13). Together, our data demonstrate the potential ability of SJPedPanel in measuring MRD and monitoring disease progression that could aid in early detection of relapse.

Discussion

We developed SJPedPanel, a hybridization capture-based assay targeting 357 pediatric specific oncogenes and tumor suppressors implicated in over 44 [see panel design section] pediatric cancer genomic studies[2-4,7,26,33,35,57,66], many through the extensive efforts of the Pediatric Cancer Genome Project [1] and NCI TARGET project [3], as well as real-time clinical sequencing efforts at St. Jude Children's Research Hospital employing WGS, WES and RNA-Seq platforms [4,66]. Considering the rich dataset of WGS and the clear recognition that fusion oncoproteins are common molecular drivers of pediatric cancers, SJPedPanel includes 297 introns that contain

medRxiv preprint doi: https://doi.org/10.1101/2023.11.27.23299068; this version posted November 28, 2023. The copyright holder for this preprint (which was not certified by peer review) is the author/funder, who has granted medRxiv a license to display the preprint in perpetuity.
All rights reserved. No reuse allowed without permission.

structural variants in 94 genes, accounting for 1.438 Mbp of genomic space, as well as 0.209 Mbp for detecting promoter-hijacking SVs. Furthermore, 7590 common SNPs are covered, allowing for the detection of copy number changes and loss of heterozygosity (LOH) at a resolution of ~1Mb. Taking into account the clear differences in the genomic landscape of cancers in children and adults, SJPedPanel has unique coverage of 110 genes frequently implicated in pediatric cancers when compared to other commonly used panels (FoundationOne Heme, FoundationOne CDx, MSK-IMPACT, OncoKids and Oncomine Comprehensive Assay v3).

We used *in silico* and experimental strategies to evaluate the performance of SJPedPanel for detecting clinically relevant somatic mutations. Using the previously published G4K study, SJPedPanel was found to cover 86% of the reported somatic markers, including SNV, Indel and SV. Similar findings were obtained by using real-time clinical sequencing samples [4,66] in which 355 (89.6%) of the 396 reported clinically relevant variants were detected in 113 cases, including all SNVs, Indels and ITDs. At patient level, at least one variant was detected in 109 out of 113 cases (median 3). These findings establish and confirm the ability of SJPedPanel to detect clinically relevant somatic mutations in a wide range of samples from a real-time clinical genomics setting for childhood cancers.

While tumor-normal paired whole genome sequencing remains the gold standard for cancer diagnostics, the overall cost and required bioinformatic pipelines and infrastructure currently limits its broad application. On the other hand, gene-panel based genomics testing can enable many centers to perform NGS-based cancer diagnostics due to the overall lower cost and faster turn-around time. The content and design of SJPedPanel allows for more comprehensive detection of the alterations common in pediatric cancer compared to both WES and other standard panels. An inherent limitation of DNA sequencing panels is the lack of coverage at all critical loci or newly discovered recurrent alterations; however, panel content can readily be updated. For example, the current version of SJPedPanel lacks sufficient coverage to identify the recurrent *ASPSCR1::TFE3* fusion characteristic of alveolar soft part sarcoma or *SSX1*/*SSX2*::*SS18* in synovial sarcoma. Such genes will be incorporated in future versions of SJPedPanel. To maximize the utility of this panel,

medRxiv preprint doi: https://doi.org/10.1101/2023.11.27.23299068; this version posted November 28, 2023. The copyright holder for this preprint (which was not certified by peer review) is the author/funder, who has granted medRxiv a license to display the preprint in perpetuity.
All rights reserved. No reuse allowed without permission.

the targeted genomic locations are included in Supplementary Tables ST1 and ST2 (Additional file 1) and future updates will be readily available upon request.

As a proof-of-principle, we demonstrate the application of using SJPedPanel for minimal residual disease (MRD) detection and post-treatment disease monitoring. It would be interesting to see the clinical value of this application using large patient cohorts in future. Because this is a pan-cancer gene panel for childhood malignancies, it will be relatively easy to develop sub panels dedicated to certain cancer subtypes to further reduce the size of the panel, and in turn enabling much higher depth with a similar cost. We expect many potential impacts on the management of childhood cancers using SJPedPanel.

Conclusions

Overall, SJPedPanel enables the detection of clinically relevant genetic alterations including rearrangements responsible for subtype-defining fusions for childhood cancers by targeted sequencing of ~0.15% of human genome. Our panel will significantly enhance the analysis of specimens with low tumor burdens for cancer monitoring and early detection.

Material and Methods

Panel design

Based on extensive research and literature review of pan cancer genome profiling studies a list of exonic and/or intronic regions (n=5009 regions, 2.82 Mbp) from 357 genes that were frequently implicated in pediatric cancers was compiled to detect single nucleotide variants (SNVs), small insertions & deletions (Indels), gene fusions, structural variants (SVs), and internal tandem duplications (ITDs). We also curated a list of 7590 single nucleotide polymorphic markers (SNPs) evenly spread across human chromosomes to detect large genomic structural rearrangements such as copy number variations (CNVs) and loss of heterozygosity (LOH). The details of all the genomics regions and SNPs used to assemble the pediatric pan cancer, termed as SJPedPanel, are available in Additional file 1: Supplementary Tables ST1 and ST2.

medRxiv preprint doi: https://doi.org/10.1101/2023.11.27.23299068; this version posted November 28, 2023. The copyright holder for this preprint (which was not certified by peer review) is the author/funder, who has granted medRxiv a license to display the preprint in perpetuity.
All rights reserved. No reuse allowed without permission.

Capture efficiency of the SJPedPanel

The high and low depth targeted enriched NGS libraries, two each, were prepared with probes designed for regions in the SJPedPanel using COLO829 BL cell line samples. Each combination of high and low depth libraries was sequenced on Illumina NovaSeq and NextSeq platforms. The data generated was used to evaluate the capture performance of the probes and uniformity of coverage across regions and loci of the SJPedPanel.

Dilution experiment

A dilution experiment using 6 cancer cell lines (ME-1, 697, Rh30, EW-8, K562, Molm13) and a non-cancer cell line (GM12878) was designed to achieve seven tumor concentrations with two replicates each. The seven dilutions were divided in three groups a) ultra-low (0.1%, 0.2%), b) low (0.5%, 1%), and c) medium (2.5%, 5% and 10%), which were sequenced at depths of 10,000X, 5000X and 2500X respectively. The cell lines were also sequenced independently in undiluted forms at 25,000X to estimate the original allele fractions of 26 cell line specific markers (14 SNVs, 4 Indels, 8 SVs) given in Additional file 1: Table ST20. Recall rate of these known markers across different dilutions was used to assess the limit of detection of the SJPedPanel.

The limit of detection (LoD) is determined by two critical factors: 1) the sequencing depth (also known as power) and 2) the noise level. For example, if the true allele fraction is 1%, a sequencing depth of 913× will ensure 95% chance of detecting this variant with >=5 mutant alleles [69]. In consideration of the high range of dilution concentrations, we aimed for 2500× depth for dilution ladders >1%, 5000× for ladders 0.5% and 1%, and 10000× for ladders 0.1% and 0.2%. On the other hand, the noise level is typically regarded as background error rate. Mutations with higher background error rates are more difficult to detect because the true signal can be overwhelmed by the background noises. We previously developed computational error suppression methods to achieve error rate of ~10^{-6}-10^{-4} for substitutions [80] and similar methods and results have been achieved for Indels and SVs (companion manuscript)

A “rotation control” method [70] was used to obtain the background count of the variants and Q-values were used to assess the statistical significance of detection

medRxiv preprint doi: https://doi.org/10.1101/2023.11.27.23299068; this version posted November 28, 2023. The copyright holder for this preprint (which was not certified by peer review) is the author/funder, who has granted medRxiv a license to display the preprint in perpetuity.
All rights reserved. No reuse allowed without permission.

based on binomial testing. All the statistical analyses were performed using R v4.0.3 (https://www.r-project.org/).

In silico down sampling experiment

We also performed *in silico* down sampling of data from a set of cancer cell line dilution samples to find out the trade-off between recall rate, down sampled depth of sequencing and associated cost estimates. The samples originally sequenced at 2500X were further down sampled to simulate depths of sequencing at 1000X, 1500X and 2000X, whereas the samples which were sequenced at 5000X and 10000X were down sampled to simulate depths of sequencing at 1000X, 1500X, 2000X, 3000X. For each of the desired down sized depth, 10 samples were simulated, each consisting of the randomly sampled reads at loci of 14 SNVs. The down sized samples were used to determine the trade-off between recall rate and depth of sequencing.

Analytical sensitivity using clinical samples

We selected 113 specimens from previously sequenced pediatric cancer cases treated at St. Jude Children's Research Hospital to represent a wide range of cancer subtypes common in pediatrics. Samples were chosen primarily from the pilot study cohort (n=40) [4] and G4K studies (n=73) [66] and had previously reported clinically relevant markers identified by triple platform approach of whole genome, whole exome, and transcriptome sequencing. The recall rate of clinically relevant markers from these cases was used to establish the analytical validity of the SJPedPanel. A list of cases and their cancer subtypes used for these purposes is provided in the (Additional file 1: Table ST11). This study was approved by the institutional review board (IRB). All patient samples are de-identified using SJID.

Library preparation, capture, and sequencing

DNA samples were obtained and subjected to DNA-seq library preparation and target enrichment followed by sequencing in the Clinical genomics laboratory as described below. An input of 100ng of DNA was used to construct libraries using the Twist Library Preparation Enzymatic Fragmentation (EF) Kit 2.0 (Twist Biosciences, CA) following the manufacturer's instructions. Capture oligos were designed to detect putative SNVs, Indels, SVs, ITDs and CNVs in 357 genes of clinical interest.

medRxiv preprint doi: https://doi.org/10.1101/2023.11.27.23299068; this version posted November 28, 2023. The copyright holder for this preprint (which was not certified by peer review) is the author/funder, who has granted medRxiv a license to display the preprint in perpetuity.
All rights reserved. No reuse allowed without permission.

SJPedPanel was synthesized at Twist Biosciences and is described in detail in the section on panel design. Eight libraries were pooled at a time and target enrichment for the SJPedPanel baits was carried out using Twist hybrid capture protocol following manufacturer's instruction. Paired-end 150-cycle sequencing was performed on NovaSeq or NextSeq instruments (Illumina Inc, CA) as appropriate. Where necessary, additional sequencing was performed to ensure that a sequencing depth of at least 1000X was achieved in all cases.

Early detection of relapsed AML cases

To test the panel's capability for disease monitoring, two cases of pediatric AML (SJAML016582 and SJAML016551) with material available at diagnosis, relapse, and remission timepoints were analyzed. Both samples provide multiple trackable somatic markers, including structural variants and SNVs. Samples were subjected to deeper sequencing depths of >5000X after targeted capture to ensure detection of low-level variants at <1%.

Generally, tumor burden is estimated using number of somatic non-synonymous mutations per Mbp region. For the sake of simplicity, in these cases, we used average VAF% of somatic variants chosen for tracking of AML at respective timepoints.

Coverage comparison between SJPedPanel and Whole exome sequencing

The content of SJPedPanel was compared with that of whole exome sequencing (WES) manifest to highlight the differences in coverage of hg19 genomic regions. An Illumina Exome 2.0 Plus hg19 BED file (Available from https://support.illumina.com/downloads/Illumina-dna-prep-exome-20-bed-files.html; last date of access: June 22, 2023) padded with 10 bp was used for region intersection analyses. We utilized recently reported somatic variants from the Genomes for Kids (G4K), a prospective nontherapeutic three-platform sequencing study of 309 patients with pediatric cancer treated at St. Jude Children's Research Hospital (Memphis, TN) [66] to assess the in silico coverage and case level concordance rates of reported variants using SJPedPanel and WES.

medRxiv preprint doi: https://doi.org/10.1101/2023.11.27.23299068; this version posted November 28, 2023. The copyright holder for this preprint (which was not certified by peer review) is the author/funder, who has granted medRxiv a license to display the preprint in perpetuity.
All rights reserved. No reuse allowed without permission.

Comparison of SJPedPanel with other panels

We also compared the content of the SJPedPanel with DNA content of five other commercially available panels such as FoundationOne® Heme, FoundationOne® CDx [53,54] by Foundation Medicine Inc., MSK-IMPACT® [6,55] by Memorial Sloan Kettering Cancer Center, OncoKids® [5] by Children's Hospital Los Angeles and Oncomine™ Comprehensive Assay v3 by Thermo Fisher Scientific Inc. [56]. These panels collectively represent breadth and diversity of clinical gene panels. Since most of the providers do not provide the exact coordinates of the regions in the panel, we compared the DNA content of these panels using standardized gene names with the help of official gene symbols and synonyms from the NCBI gene database (https://www.ncbi.nlm.nih.gov/gene, last accessed on March 10, 2023).

Bioinformatics analyses

The adapter trimmed paired end FASTQ files generated on the Illumina NovaSeq/NextSeq platforms were assessed for sequence quality using FastQC v0.11.9 and SequencErr v2.0.9 [75]. The reads were mapped against GRCh37 build using BWA mem 0.7.12-r1039 [81]. The utility commands in SAMtools v1.7 and bedtools v2.25.0 were used perform simple operations using BAM and BED files. The count files obtained from BAM files using SequencErr were further passed as an input to DeepSeqCoverageQC v0.3.1 (Available from GitHub: https://github.com/pandurang-kolekar/DeepSeqCoverageQC) to compute depth of coverage QC metrics of the sequenced samples over loci/regions of the SJPedPanel. The genotyping of SVs and Indels to compute the allele fractions was carried out using in-house scripts (https://github.com/stjude/SVIndelGenotyper). The CNVs were detected using CNVkit v0.9.10 [82]. The BAM files of 30 germline samples were used to create a pooled reference of per-bin copy number estimates. The segment & bin-level call files along with CNV diagrams generated by CNVkit batch command were used to review the CNV calls in tumor samples. To determine the LOH in sequenced samples, the minor allele frequencies of 7590 SNPs were computed using count files generated by SequencErr and subsequently used to generate allelic imbalance plots over chromosomes. The output files and diagrams generated by CNVkit v0.9.10 and the allelic imbalance figures used to review CNV and LOH events are available from GitHub repository at https://github.com/XMaLab/SJPedPanel_Supplementary_Data

medRxiv preprint doi: https://doi.org/10.1101/2023.11.27.23299068; this version posted November 28, 2023. The copyright holder for this preprint (which was not certified by peer review) is the author/funder, who has granted medRxiv a license to display the preprint in perpetuity.
All rights reserved. No reuse allowed without permission.

References

1 Downing, J. R. *et al.* The Pediatric Cancer Genome Project. *Nat Genet* **44**, 619-622, doi:10.1038/ng.2287 (2012).
2 Grobner, S. N. *et al.* The landscape of genomic alterations across childhood cancers. *Nature* **555**, 321-327, doi:10.1038/nature25480 (2018).
3 Ma, X. *et al.* Pan-cancer genome and transcriptome analyses of 1,699 paediatric leukaemias and solid tumours. *Nature* **555**, 371-376, doi:10.1038/nature25795 (2018).
4 Rusch, M. *et al.* Clinical cancer genomic profiling by three-platform sequencing of whole genome, whole exome and transcriptome. *Nat Commun* **9**, 3962, doi:10.1038/s41467-018-06485-7 (2018).
5 Hiemenz, M. C. *et al.* OncoKids: A Comprehensive Next-Generation Sequencing Panel for Pediatric Malignancies. *J Mol Diagn* **20**, 765-776, doi:10.1016/j.jmoldx.2018.06.009 (2018).
6 Cheng, D. T. *et al.* Memorial Sloan Kettering-Integrated Mutation Profiling of Actionable Cancer Targets (MSK-IMPACT): A Hybridization Capture-Based Next-Generation Sequencing Clinical Assay for Solid Tumor Molecular Oncology. *J Mol Diagn* **17**, 251-264, doi:10.1016/j.jmoldx.2014.12.006 (2015).
7 Liu, Y. *et al.* Etiology of oncogenic fusions in 5,190 childhood cancers and its clinical and therapeutic implication. *Nat Commun* **14**, 1739, doi:10.1038/s41467-023-37438-4 (2023).
8 Cheung, N. K. *et al.* Association of age at diagnosis and genetic mutations in patients with neuroblastoma. *JAMA* **307**, 1062-1071, doi:10.1001/jama.2012.228 (2012).
9 Gruber, T. A. *et al.* An Inv(16)(p13.3q24.3)-encoded CBFA2T3-GLIS2 fusion protein defines an aggressive subtype of pediatric acute megakaryoblastic leukemia. *Cancer Cell* **22**, 683-697, doi:10.1016/j.ccr.2012.10.007 (2012).
10 Roberts, K. G. *et al.* Genetic alterations activating kinase and cytokine receptor signaling in high-risk acute lymphoblastic leukemia. *Cancer Cell* **22**, 153-166, doi:10.1016/j.ccr.2012.06.005 (2012).
11 Robinson, G. *et al.* Novel mutations target distinct subgroups of medulloblastoma. *Nature* **488**, 43-48, doi:10.1038/nature11213 (2012).
12 Wu, G. *et al.* Somatic histone H3 alterations in pediatric diffuse intrinsic pontine gliomas and non-brainstem glioblastomas. *Nat Genet* **44**, 251-253, doi:10.1038/ng.1102 (2012).
13 Zhang, J. *et al.* A novel retinoblastoma therapy from genomic and epigenetic analyses. *Nature* **481**, 329-334, doi:10.1038/nature10733 (2012).
14 Zhang, J. *et al.* The genetic basis of early T-cell precursor acute lymphoblastic leukaemia. *Nature* **481**, 157-163, doi:10.1038/nature10725 (2012).
15 Chen, X. *et al.* Targeting oxidative stress in embryonal rhabdomyosarcoma. *Cancer Cell* **24**, 710-724, doi:10.1016/j.ccr.2013.11.002 (2013).
16 Holmfeldt, L. *et al.* The genomic landscape of hypodiploid acute lymphoblastic leukemia. *Nat Genet* **45**, 242-252, doi:10.1038/ng.2532 (2013).
17 Jaffe, J. D. *et al.* Global chromatin profiling reveals NSD2 mutations in pediatric acute lymphoblastic leukemia. *Nat Genet* **45**, 1386-1391, doi:10.1038/ng.2777 (2013).
18 Paugh, B. S. *et al.* Novel oncogenic PDGFRA mutations in pediatric high-grade gliomas. *Cancer Res* **73**, 6219-6229, doi:10.1158/0008-5472.CAN-13-1491 (2013).
19 Shah, S. *et al.* A recurrent germline PAX5 mutation confers susceptibility to pre-B cell acute lymphoblastic leukemia. *Nat Genet* **45**, 1226-1231, doi:10.1038/ng.2754 (2013).
20 Zhang, J. *et al.* Whole-genome sequencing identifies genetic alterations in pediatric low-grade gliomas. *Nat Genet* **45**, 602-612, doi:10.1038/ng.2611 (2013).
21 Chen, X. *et al.* Recurrent somatic structural variations contribute to tumorigenesis in pediatric osteosarcoma. *Cell Rep* **7**, 104-112, doi:10.1016/j.celrep.2014.03.003 (2014).
22 Parker, M. *et al.* C11orf95-RELA fusions drive oncogenic NF-kappaB signalling in ependymoma. *Nature* **506**, 451-455, doi:10.1038/nature13109 (2014).
23 Roberts, K. G. *et al.* Targetable kinase-activating lesions in Ph-like acute lymphoblastic leukemia. *N Engl J Med* **371**, 1005-1015, doi:10.1056/NEJMoa1403088 (2014).
24 Tirode, F. *et al.* Genomic landscape of Ewing sarcoma defines an aggressive subtype with co-association of STAG2 and TP53 mutations. *Cancer Discov* **4**, 1342-1353, doi:10.1158/2159-8290.CD-14-0622 (2014).
25 Wu, G. *et al.* The genomic landscape of diffuse intrinsic pontine glioma and pediatric non-brainstem high-grade glioma. *Nat Genet* **46**, 444-450, doi:10.1038/ng.2938 (2014).

medRxiv preprint doi: https://doi.org/10.1101/2023.11.27.23299068; this version posted November 28, 2023. The copyright holder for this preprint (which was not certified by peer review) is the author/funder, who has granted medRxiv a license to display the preprint in perpetuity.
All rights reserved. No reuse allowed without permission.

26 Andersson, A. K. *et al.* The landscape of somatic mutations in infant MLL-rearranged acute lymphoblastic leukemias. *Nat Genet* **47**, 330-337, doi:10.1038/ng.3230 (2015).
27 Li, B. *et al.* Negative feedback-defective PRPS1 mutants drive thiopurine resistance in relapsed childhood ALL. *Nat Med* **21**, 563-571, doi:10.1038/nm.3840 (2015).
28 Lu, C. *et al.* The genomic landscape of childhood and adolescent melanoma. *J Invest Dermatol* **135**, 816-823, doi:10.1038/jid.2014.425 (2015).
29 Ma, X. *et al.* Rise and fall of subclones from diagnosis to relapse in pediatric B-acute lymphoblastic leukaemia. *Nat Commun* **6**, 6604, doi:10.1038/ncomms7604 (2015).
30 Pinto, E. M. *et al.* Genomic landscape of paediatric adrenocortical tumours. *Nat Commun* **6**, 6302, doi:10.1038/ncomms7302 (2015).
31 Tong, Y. *et al.* Cross-Species Genomics Identifies TAF12, NFYC, and RAD54L as Choroid Plexus Carcinoma Oncogenes. *Cancer Cell* **27**, 712-727, doi:10.1016/j.ccell.2015.04.005 (2015).
32 Zhang, J. *et al.* Germline Mutations in Predisposition Genes in Pediatric Cancer. *N Engl J Med* **373**, 2336-2346, doi:10.1056/NEJMoa1508054 (2015).
33 Faber, Z. J. *et al.* The genomic landscape of core-binding factor acute myeloid leukemias. *Nat Genet* **48**, 1551-1556, doi:10.1038/ng.3709 (2016).
34 Iacobucci, I. *et al.* Truncating Erythropoietin Receptor Rearrangements in Acute Lymphoblastic Leukemia. *Cancer Cell* **29**, 186-200, doi:10.1016/j.ccell.2015.12.013 (2016).
35 Liu, Y. F. *et al.* Genomic Profiling of Adult and Pediatric B-cell Acute Lymphoblastic Leukemia. *EBioMedicine* **8**, 173-183, doi:10.1016/j.ebiom.2016.04.038 (2016).
36 Zhang, J. *et al.* Deregulation of DUX4 and ERG in acute lymphoblastic leukemia. *Nat Genet* **48**, 1481-1489, doi:10.1038/ng.3691 (2016).
37 de Rooij, J. D. *et al.* Pediatric non-Down syndrome acute megakaryoblastic leukemia is characterized by distinct genomic subsets with varying outcomes. *Nat Genet* **49**, 451-456, doi:10.1038/ng.3772 (2017).
38 Liu, Y. *et al.* The genomic landscape of pediatric and young adult T-lineage acute lymphoblastic leukemia. *Nat Genet* **49**, 1211-1218, doi:10.1038/ng.3909 (2017).
39 Northcott, P. A. *et al.* The whole-genome landscape of medulloblastoma subtypes. *Nature* **547**, 311-317, doi:10.1038/nature22973 (2017).
40 Alexander, T. B. *et al.* The genetic basis and cell of origin of mixed phenotype acute leukaemia. *Nature* **562**, 373-379, doi:10.1038/s41586-018-0436-0 (2018).
41 Bolouri, H. *et al.* The molecular landscape of pediatric acute myeloid leukemia reveals recurrent structural alterations and age-specific mutational interactions. *Nat Med* **24**, 103-112, doi:10.1038/nm.4439 (2018).
42 Pajtler, K. W. *et al.* Molecular heterogeneity and CXorf67 alterations in posterior fossa group A (PFA) ependymomas. *Acta Neuropathol* **136**, 211-226, doi:10.1007/s00401-018-1877-0 (2018).
43 Stewart, E. *et al.* Identification of Therapeutic Targets in Rhabdomyosarcoma through Integrated Genomic, Epigenomic, and Proteomic Analyses. *Cancer Cell* **34**, 411-426 e419, doi:10.1016/j.ccell.2018.07.012 (2018).
44 Brady, S. W. *et al.* The Clonal Evolution of Metastatic Osteosarcoma as Shaped by Cisplatin Treatment. *Mol Cancer Res* **17**, 895-906, doi:10.1158/1541-7786.MCR-18-0620 (2019).
45 Newman, S. *et al.* Clinical genome sequencing uncovers potentially targetable truncations and fusions of MAP3K8 in spitzoid and other melanomas. *Nat Med* **25**, 597-602, doi:10.1038/s41591-019-0373-y (2019).
46 Brady, S. W. *et al.* Pan-neuroblastoma analysis reveals age- and signature-associated driver alterations. *Nat Commun* **11**, 5183, doi:10.1038/s41467-020-18987-4 (2020).
47 Brady, S. W. *et al.* Therapy-induced mutagenesis in relapsed ALL is supported by mutational signature analysis. *Blood* **136**, 2235-2237, doi:10.1182/blood.2020008107 (2020).
48 Waanders, E. *et al.* Mutational landscape and patterns of clonal evolution in relapsed pediatric acute lymphoblastic leukemia. *Blood Cancer Discov* **1**, 96-111, doi:10.1158/0008-5472.BCD-19-0041 (2020).
49 Zhou, X. *et al.* Exploring genomic alteration in pediatric cancer using ProteinPaint. *Nat Genet* **48**, 4-6, doi:10.1038/ng.3466 (2016).
50 Zhou, X. *et al.* Exploration of Coding and Non-coding Variants in Cancer Using GenomePaint. *Cancer Cell* **39**, 83-95 e84, doi:10.1016/j.ccell.2020.12.011 (2021).
51 Ottema, S. *et al.* The leukemic oncogene EVI1 hijacks a MYC super-enhancer by CTCF-facilitated loops. *Nat Commun* **12**, 5679, doi:10.1038/s41467-021-25862-3 (2021).

medRxiv preprint doi: https://doi.org/10.1101/2023.11.27.23299068; this version posted November 28, 2023. The copyright holder for this preprint (which was not certified by peer review) is the author/funder, who has granted medRxiv a license to display the preprint in perpetuity.
All rights reserved. No reuse allowed without permission.

52 Northcott, P. A. *et al.* Enhancer hijacking activates GFI1 family oncogenes in medulloblastoma. *Nature* **511**, 428-434, doi:10.1038/nature13379 (2014).
53 *Foundation One Heme*, <https://assets.ctfassets.net/w98cd481qyp0/42r1cTE8VR4137CaHrsaen/baf91080cb3d78a52ada10c6358fa130/FoundationOne_Heme_Technical_Specifications.pdf> (2019).
54 *Foundation One CDX*, <https://assets.ctfassets.net/w98cd481qyp0/YqqKHaqQmFeqc5ueQk48w/d12f19680205941ea3fee417f08e9524/F1CDx_Technical_Specifications.pdf> (2022).
55 *MSK-IMPACT Panel*, <https://www.accessdata.fda.gov/cdrh_docs/reviews/den170058.pdf> (2017).
56 *Thermo Fisher Oncomine Comprehensive Assay v3*, <https://assets.thermofisher.com/TFS-Assets/LSG/brochures/oncomine-comprehensive-assay-v3-flyer.pdf> (2022).
57 Gadd, S. *et al.* A Children's Oncology Group and TARGET initiative exploring the genetic landscape of Wilms tumor. *Nat Genet* **49**, 1487-1494, doi:10.1038/ng.3940 (2017).
58 DeSouza, R. M., Jones, B. R., Lowis, S. P. & Kurian, K. M. Pediatric medulloblastoma - update on molecular classification driving targeted therapies. *Front Oncol* **4**, 176, doi:10.3389/fonc.2014.00176 (2014).
59 Arabzade, A. *et al.* ZFTA-RELA Dictates Oncogenic Transcriptional Programs to Drive Aggressive Supratentorial Ependymoma. *Cancer Discov* **11**, 2200-2215, doi:10.1158/2159-8290.CD-20-1066 (2021).
60 Umeda, M. *et al.* Integrated Genomic Analysis Identifies UBTF Tandem Duplications as a Recurrent Lesion in Pediatric Acute Myeloid Leukemia. *Blood Cancer Discov* **3**, 194-207, doi:10.1158/2643-3230.BCD-21-0160 (2022).
61 Jeha, S. *et al.* Clinical significance of novel subtypes of acute lymphoblastic leukemia in the context of minimal residual disease-directed therapy. *Blood Cancer Discov* **2**, 326-337, doi:10.1158/2643-3230.BCD-20-0229 (2021).
62 He, J. *et al.* Integrated genomic DNA/RNA profiling of hematologic malignancies in the clinical setting. *Blood* **127**, 3004-3014, doi:10.1182/blood-2015-08-664649 (2016).
63 Conway, J. R., Lex, A. & Gehlenborg, N. UpSetR: an R package for the visualization of intersecting sets and their properties. *Bioinformatics* **33**, 2938-2940, doi:10.1093/bioinformatics/btx364 (2017).
64 Craig, D. W. *et al.* A somatic reference standard for cancer genome sequencing. *Sci Rep* **6**, 24607, doi:10.1038/srep24607 (2016).
65 Pleasance, E. D. *et al.* A comprehensive catalogue of somatic mutations from a human cancer genome. *Nature* **463**, 191-196, doi:10.1038/nature08658 (2010).
66 Newman, S. *et al.* Genomes for Kids: The Scope of Pathogenic Mutations in Pediatric Cancer Revealed by Comprehensive DNA and RNA Sequencing. *Cancer Discov* **11**, 3008-3027, doi:10.1158/2159-8290.CD-20-1631 (2021).
67 Gu, Z. *et al.* PAX5-driven subtypes of B-progenitor acute lymphoblastic leukemia. *Nat Genet* **51**, 296-307, doi:10.1038/s41588-018-0315-5 (2019).
68 Choi, S. M., Dewar, R., Burke, P. W. & Shao, L. Partial tandem duplication of KMT2A (MLL) may predict a subset of myelodysplastic syndrome with unique characteristics and poor outcome. *Haematologica* **103**, e131-e134, doi:10.3324/haematol.2017.185249 (2018).
69 Ma, X., Arunachalam, S. & Liu, Y. Applications of probability and statistics in cancer. *Quantitative Biology* **8**, 15-108, doi:10.1007/s40484-020-0203-8 (2020).
70 Li, B. *et al.* Therapy-induced mutations drive the genomic landscape of relapsed acute lymphoblastic leukemia. *Blood* **135**, 41-55, doi:10.1182/blood.2019002220 (2020).
71 Patel, J. P. *et al.* Prognostic relevance of integrated genetic profiling in acute myeloid leukemia. *N Engl J Med* **366**, 1079-1089, doi:10.1056/NEJMoa1112304 (2012).
72 Tyner, J. W. *et al.* Functional genomic landscape of acute myeloid leukaemia. *Nature* **562**, 526-531, doi:10.1038/s41586-018-0623-z (2018).
73 Bairoch, A. The Cellosaurus, a Cell-Line Knowledge Resource. *J Biomol Tech* **29**, 25-38, doi:10.7171/jbt.18-2902-002 (2018).
74 Tsherniak, A. *et al.* Defining a Cancer Dependency Map. *Cell* **170**, 564-576 e516, doi:10.1016/j.cell.2017.06.010 (2017).
75 Davis, E. M. *et al.* SequencErr: measuring and suppressing sequencer errors in next-generation sequencing data. *Genome Biol* **22**, 37, doi:10.1186/s13059-020-02254-2 (2021).
76 Deveson, I. W. *et al.* Evaluating the analytical validity of circulating tumor DNA sequencing assays for precision oncology. *Nat Biotechnol* **39**, 1115-1128, doi:10.1038/s41587-021-00857-z (2021).

medRxiv preprint doi: https://doi.org/10.1101/2023.11.27.23299068; this version posted November 28, 2023. The copyright holder for this preprint (which was not certified by peer review) is the author/funder, who has granted medRxiv a license to display the preprint in perpetuity.
All rights reserved. No reuse allowed without permission.

77 Loken, M. R. *et al.* Residual disease detected by multidimensional flow cytometry signifies high relapse risk in patients with de novo acute myeloid leukemia: a report from Children's Oncology Group. *Blood* **120**, 1581-1588, doi:10.1182/blood-2012-02-408336 (2012).
78 Gabert, J. *et al.* Standardization and quality control studies of 'real-time' quantitative reverse transcriptase polymerase chain reaction of fusion gene transcripts for residual disease detection in leukemia - a Europe Against Cancer program. *Leukemia* **17**, 2318-2357, doi:10.1038/sj.leu.2403135 (2003).
79 Mencia-Trinchant, N. *et al.* Minimal Residual Disease Monitoring of Acute Myeloid Leukemia by Massively Multiplex Digital PCR in Patients with NPM1 Mutations. *J Mol Diagn* **19**, 537-548, doi:10.1016/j.jmoldx.2017.03.005 (2017).
80 Ma, X. *et al.* Analysis of error profiles in deep next-generation sequencing data. *Genome Biol* **20**, 50, doi:10.1186/s13059-019-1659-6 (2019).
81 Li, H. & Durbin, R. Fast and accurate long-read alignment with Burrows-Wheeler transform. *Bioinformatics* **26**, 589-595, doi:10.1093/bioinformatics/btp698 (2010).
82 Talevich, E., Shain, A. H., Botton, T. & Bastian, B. C. CNVkit: Genome-Wide Copy Number Detection and Visualization from Targeted DNA Sequencing. *PLoS Comput Biol* **12**, e1004873, doi:10.1371/journal.pcbi.1004873 (2016).

Declarations

Availability of data and materials

The cell line data generated for this study have been deposited in the European Nucleotide Archive (ENA) at EMBL-EBI under accession number PRJEB64356 (https://www.ebi.ac.uk/ena/browser/view/PRJEB64356). The accession numbers of the samples are listed in Additional File 1: Supplementary Tables ST5 and ST21.

Funding

This work was supported in part by the National Cancer Institute of the National Institutes of Health under Award Number R01CA273326 (to X.M.), the Fund for Innovation in Cancer Informatics (www.the-ici-fund.org, to X.M. and J.M.K.), Cancer Center Support Grant P30CA021765 (Developmental Fund to J.M.K. and X.M.) from the National Institutes of Health, and the American Lebanese Syrian Associated Charities (ALSAC). The content is solely the responsibility of the authors and does not necessarily represent the official views of the National Institutes of Health or other funding agencies.

Authors' contributions

X.M. and J.M.K. conceived the research. P.K. collected data, performed data analyses, generated figures and implemented the *DeepSeqCoverageQC* algorithm.

medRxiv preprint doi: https://doi.org/10.1101/2023.11.27.23299068; this version posted November 28, 2023. The copyright holder for this preprint (which was not certified by peer review) is the author/funder, who has granted medRxiv a license to display the preprint in perpetuity.
All rights reserved. No reuse allowed without permission.

V.B. and L.D. performed sequencing experiments. J.M.K. coordinated clinical specimen acquisition. Y.L. and Q.T. implemented *SVInDelGenotyper* algorithm. P.K., V.B., L.D.,Y.L.,S.F.,Q.T.,H.M.,A.L.H,E.P.,Z.L.,J.M.,J.N,J.G,J.M.,D.P.,S.M.,L.W., E.S.,J.E.,J.M.K. and X.M. contributed to analyses. All authors read and approved the final manuscript.

Authors' information

Pandurang Kolekar, Vidya Balagopal and Li Dong contributed equally to this work.

Ethics approval and consent to participate

Informed consent was obtained from all subjects.

Competing interests

The authors declare no competing financial interests.